Period-doubling cascade to chaotic phase dynamics in Taylor vortex flow with hourglass geometry

Richard J. Wiener,[1,*] Geoffrey L. Snyder,[1] Micah P. Prange,[1] Daniel Frediani,[2] and Paul R. Diaz[2]
[1]*Department of Physics, Pacific University, Forest Grove, Oregon 97116*
[2]*Department of Physics, Lewis and Clark College, Portland, Oregon 97219*
(Received 23 September 1996)

We report on an experimental investigation of a ramp-induced Eckhaus instability, a mechanism which creates a period-doubling cascade to spatiotemporal chaos in a quasi-one-dimensional pattern-forming system. This previously experimentally unexplored mechanism for the generation of chaos involves the phase diffusion of a cellular pattern, resulting from a subcritical spatial ramp. If the subcritical ramp selects an Eckhaus-unstable wave number, diffusion toward this wave number triggers persistent phase slips that create (or destroy) cellular structures. Using a nonlinear phase equation to model ramp-induced Eckhaus instabilities, Riecke and Paap predicted richer-than-periodic dynamics, including spatiotemporal chaos for systems with subcritical ramps satisfying certain general conditions. The specific system that we investigated is a variation of Taylor vortex flow, with the inner cylinder replaced by an hourglass geometry, which satisfies the model conditions for a subcritical ramp that generates chaos. We observed a period-doubling cascade to chaotic phase slips, in qualitative agreement with the predictions of Riecke and Paap. [S1063-651X(97)01005-2]

PACS number(s): 47.54.+r, 47.52.+j, 47.20.Ky

I. INTRODUCTION

Since Pomeau and Manneville first proposed using a phase equation to model the dynamics of patterns in forced dissipative systems, the phase-dynamics approach has met with impressive success [1]. The underlying basis for phase dynamics is that diffusive behavior for the phase of a spatially varying pattern is characteristic of a variety of pattern-forming systems. An example is the diffusive propagation of a phase modulation at one boundary through the interior of a one-dimensional pattern [2,3]. Phase equations can be used to describe the dynamics of phase diffusion and such equations are an important example of reduced nonlinear equations, which are simpler than and systematically derivable from more fundamental (e.g., Navier-Stokes) equations [4].

A particularly intriguing example of phase dynamics is its application to spatially *inhomogeneous* quasi-one-dimensional systems, where a control parameter R (which determines the strength of the external driving) is varied in space so that part of the system is subcritical, $R<R_c$, a so-called subcritical ramp. Kramer *et al.* showed theoretically and Dominguez-Lerma and co-workers confirmed experimentally that subcritical ramps select unique patterns in quasi-one-dimensional systems; a distinct wave number q for a spatially periodic pattern results from a specific spatial variation of R [5–7]. This contrasts with patterns in systems with no spatial variation in R, for which there always exists a stable *band* of wave numbers at a given R. Thus nonuniqueness of patterns, which is a distinct feature of homogeneous nonlinear systems, is no longer characteristic of inhomogeneous systems. Riecke and Paap demonstrated the strength of the phase-dynamics approach by using a phase equation to quantitatively calculate uniquely selected wave numbers in subcritically ramped systems [8,9].

The particular forced dissipative system investigated by Dominguez-Lerma and co-workers is Taylor-Couette flow, the flow of fluid between concentric rotating cylinders. This flow is a structureless shear flow, referred to as *circular Couette flow* (CCF), when the inner cylinder rotates at small values of the Reynolds number R (the system's control parameter) and the outer cylinder is stationary. At $R=R_c$ the system undergoes a steady supercritical bifurcation from patternless CCF to a spatially periodic quasi-one-dimensional pattern of toroidal vortices, known as *Taylor vortex flow* (TVF) [10,11]. This pattern has a finite band of stable wave numbers that varies in width with R. At the boundaries of this band, the wave number q becomes unstable to long wavelength modulations and this instability, known as the Eckhaus instability, is a generic feature of stationary patterns [12]. If the wavelength of Taylor vortex pairs is either compressed or stretched beyond the Eckhaus-stable limit, a *phase slip* occurs, in which there is a loss or gain of a vortex pair, which is one wavelength of the pattern. The phase slip restores the pattern to within the Eckhaus-stable band of wave numbers.

The spatial homogeneity of the Taylor-Couette system can be broken by replacing the inner or outer cylinder (or both) with a ''cylinder'' which has a straight section and a ramped section over which its radius varies. This creates a spatial variation in R, since R depends on the radii of the inner and outer cylinders. For particular spatial ramps there is a range of driving over which it is possible to have TVF in the straight section and in part of the ramped section and CCF in the rest of the ramped section, i.e., a subcritical ramp. The wave number q of the pattern varies over the supercritical region of the ramped section and is constant over the supercritical interior (except near the ramp), where R does not vary spatially. Subcritical ramps create nearly unique patterns and in the limit of infinitesimal ramp angles

*Electronic address: wienerr@pacificu.edu

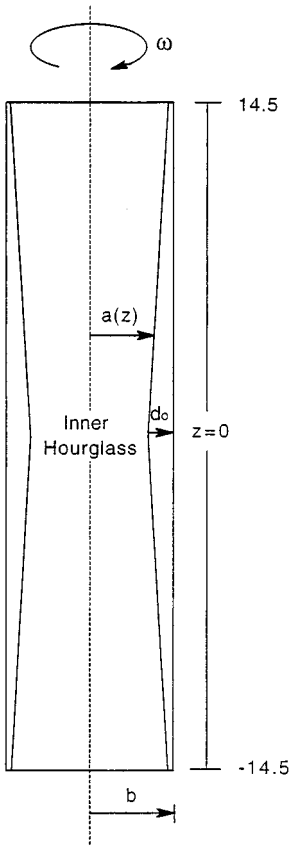

FIG. 1. Schematic cross section of the hourglass geometry.

a single wave number is selected for the interior of the system. The particular q which is selected depends on the details of the ramp and on the spatially varying control parameter R [6–9].

Remarkably, it is possible to construct particular subcritical ramps that select unique *unstable* wave numbers, i.e., wave numbers which lie *outside* the Eckhaus-stable band for the homogeneous system. Riecke and Paap used the phase-dynamics approach to predict that the ramp-induced selection of an Eckhaus-unstable wave number creates a pattern with persistent dynamics, rather than a stationary pattern [8,9,13]. Ning, Ahlers, and Cannell confirmed this prediction experimentally by showing that the selection of an unstable state by a subcritical ramp leads to periodic phase slips in the homogeneous interior of the system [14]. In their experiment, a vortex pair is periodically destroyed in the interior and replenished by axially drifting vortices that move through the ramped section toward the interior. The measured drift frequency agrees quantitatively with the predictions made by Riecke and Paap, using a phase equation with no adjustable parameters [8,9,14].

At the *Seventh International Couette-Taylor Workshop*, Riecke and Paap raised the following intriguing questions [15]: Why are the dynamics in the experiment of Ning, Ahlers, and Cannell periodic? Could one set up a system in which the dynamics become more complicated and even chaotic? Riecke and Paap conjectured that the sharp corner between the ramped and interior sections of the experimental system singles out a preferred location that constrains phase slips at the same place and, periodically, in time. To obtain

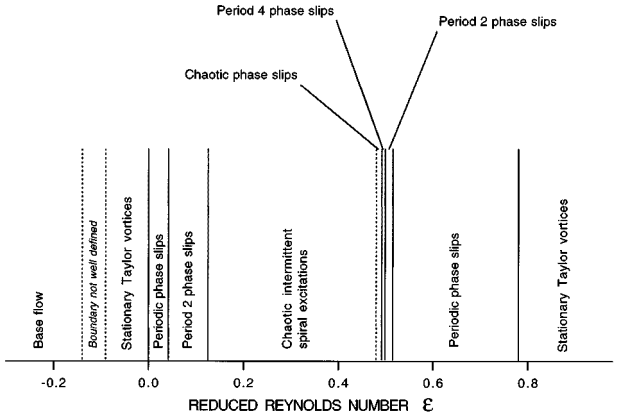

FIG. 2. Schematic transition diagram as a function of the reduced Reynolds number ε.

more complicated dynamics, the phase slips need to occur at multiple locations. Thus, a setup with continuously smooth ramps (with no sharp corners), which creates a supercritical region bounded by subcritical regions, might lead to richer dynamics, including low-dimensional spatiotemporal chaos. As a first step toward verifying this conjecture, Riecke and Paap numerically investigated the slow dynamics of a nonlinear reaction-diffusion model that can be described by a one-dimensional phase equation [15,16]. Since phase diffusion and the Eckhaus instability are characteristic of steady patterns, this model is meant to elucidate the generic dynamics in quasi-one-dimensional pattern-forming systems that have a smooth subcritical ramp that triggers phase slips. The condition for a phase slip to occur at a particular location is that the spatially dependent diffusion coefficient in the phase equation goes to zero at that location. Riecke and Paap used smooth reflection-symmetric parabolic ramps, with no homogeneous section, in two control parameters in the model. This would correspond to ramping both ''cylinders'' in the Taylor-Couette system. The reason for reflection symmetry (i.e., $z \rightarrow -z$, where z corresponds to the axial direction and $z=0$ to the axial midpoint) is to prevent a drift in the pattern that would arise from asymmetrical ramps selecting different *stable* wave numbers at the two boundaries of the supercritical region [5,17]. Such a drift might preempt a ramp-induced Eckhaus instability. Riecke and Paap found that their ramps can indeed destabilize the model pattern over several wavelengths, thereby allowing phase slips to occur at different locations. This additional freedom in the model system leads to a period-doubling cascade culminating in phase slips that occur chaotically in both time and space. The richer-than-periodic dynamics result from an interaction between competing phase-slip processes [15,16].

Can the period-doubling cascade predicted by this simple one-dimensional model be found in a real physical system, that includes the main ingredients that lead to chaos, smooth reflection-symmetric subcritical ramps that induce phase diffusion and an Eckhaus instability? In order to answer this question we designed perhaps the simplest geometry for the Taylor-Couette system that satisfies these conditions. We chose to replace only the inner cylinder with a spatially ramped geometry. This geometry, which we refer to as an *inner hourglass*, consists of two linear ramps connected smoothly at the symmetry center. The hourglass geometry is

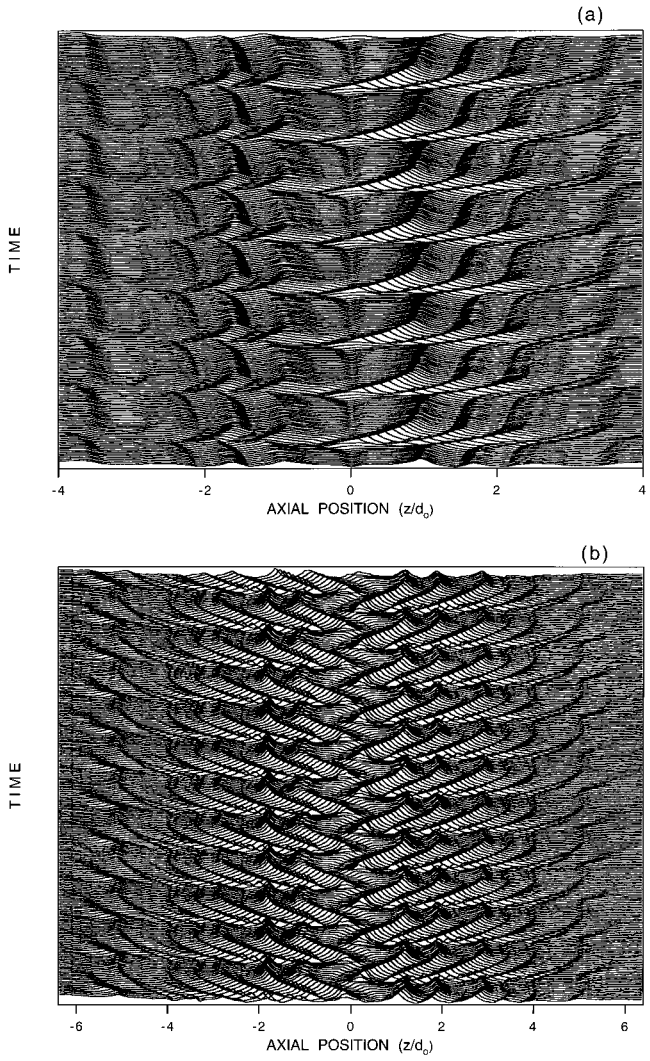

FIG. 3. Position-time diagrams of pixel intensities displaced in time at 1-s intervals: (a) periodic pattern just above onset and (b) period-two pattern at small ε.

reflection-symmetric with no homogeneous section and it allows for a range of driving over which there is TVF in the middle, bounded by subcritical flow at both ends.

In this paper we present an experimental study of the different dynamics that can be found in Taylor-Couette flow with the hourglass geometry. We concentrate on aspects of the dynamics that can be compared to predictions from the one-dimensional phase equation. We find that the hourglass ramp generates diffusive drifting of vortices and selects an Eckhaus-unstable wave number that triggers persistent phase slips. The dynamics, which are axisymmetric and, therefore, quasi-one-dimensional, can occur periodically or aperiodically and there is a sequence of period doublings (period four is the highest periodicity observed) which leads to chaotic phase slips. Thus, the selection of an *unstable* state in a pattern-forming system can create period-doubling and chaotic dynamics. Although the locations of the phase slips are chaotic in both time and space, the pattern remains spatially organized. We also find that, for a range of external driving, the system becomes unstable to spiral vortices rather than axisymmetric phase slips. This flow is interesting in that it involves intermittent axisymmetry breaking; a spiral excitation dies out until axisymmetric vortex drifting triggers a new excitation. The relationship of this flow to the chaotic dynamics and to the truncation of the period-doubling cascade at period four is discussed.

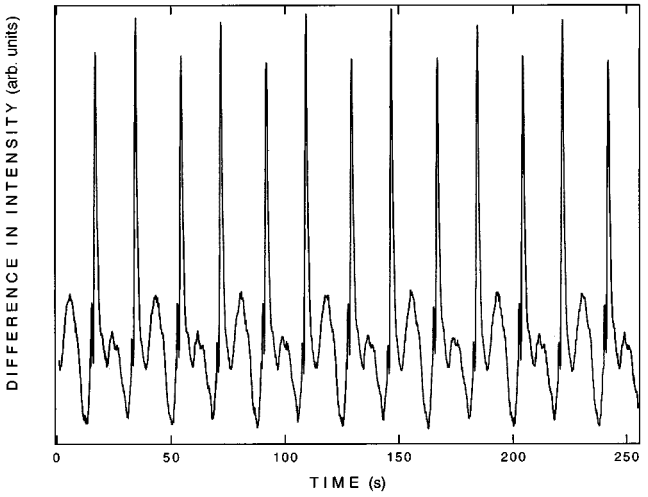

FIG. 4. Difference in intensity versus time, for a period-two regime. The maximum of a sharp peak indicates a phase slip.

II. EXPERIMENTAL SETUP

The modified Taylor-Couette apparatus used in our experiment consists of a rotating inner hourglass made of Delrin plastic, a stationary outer cylinder made from precision-bore glass with a radius $b=2.54$ cm, stationary Delrin plastic endcaps, and a glass temperature control jacket. In Fig. 1 we show a schematic cross section of the concentric inner hourglass and outer cylinder. Their mutual axis, taken as the z axis, is the axis of rotation of the inner hourglass. The inner hourglass itself consists of two linear ramps joined parabolically in the middle to form a symmetry center, defined as the $z=0$ plane. There is no discontinuity in the slope of the hourglass radius $a(z)$, which varies from 2.41 cm at the ends to $a_0=1.78$ cm at the symmetry center. Thus, the radius ratio $\eta(z)=a(z)/b$ also varies, from 0.950 at the ends to 0.700 at $z=0$. The angle of the linear ramps $\alpha=0.057$ rad. The length L of the hourglass between the endcaps in the axial direction is 22.1 cm. The gap size at the symmetry center, where it is greatest, is $d_0=b-a_0=0.760$ cm. This gives a dimensionless length of $\Gamma=L/d_0=29.1$. The axial coordinate z is also scaled in terms of d_0. The strength of the external driving is determined by the Reynolds number $R(z)=a(z)\omega d(z)/\nu$, where ω is the angular speed of the inner hourglass and ν is the kinematic viscosity of the experimental fluid. The inner hourglass is driven by a computer-controlled stepper motor which is precise to 0.001 Hz. The experimental fluid is a water-glycerol mixture with a 1.5%, by volume, Kalliroscope suspension of polymeric flakes, added for flow visualization [18]. In order to maintain constant viscosity, the temperature of the fluid is regulated to within 0.1 K by circulating thermostatically controlled water through the temperature control jacket surrounding the outer cylinder. Data acquisition is achieved by gathering light reflected off Kalliroscope flakes onto a charge-coupled-device camera which is connected to a

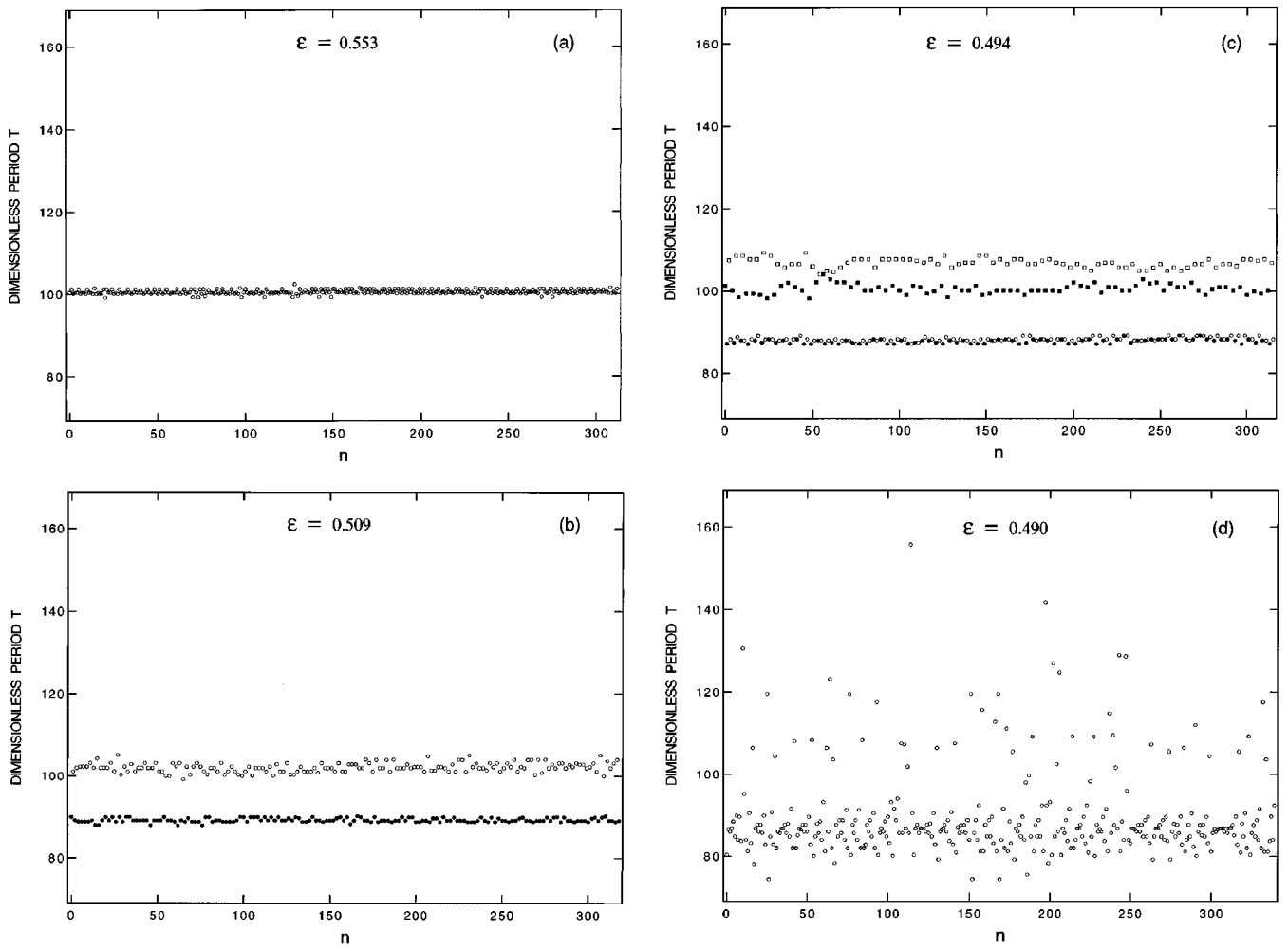

FIG. 5. Dimensionless period T for the time between the nth$+1$ and nth phase slips plotted against n for (a) periodic, (b) period-two, (c) period-four, and (d) chaotic dynamics. See text for meaning of symbols.

computer-controlled frame grabber with a grabbing resolution of 512×486 pixels and a gray-scale resolution of 8 bits (256 shades).

Since the transition to time-dependent phase slips is precisely detectable, unlike the transition to TVF (see Sec. III), we chose to define a reduced Reynolds number ε in terms of ω_{ps}, the critical angular speed for the onset of phase slips: $\varepsilon=(\omega/\omega_{ps})-1$. Note that this expression for ε is valid only if the viscosity-dependent ω_{ps} is held constant. In order to guarantee this condition, our protocol was to determine $\omega_{ps}/2\pi$ to within at least ±0.01 Hz, sometimes to within ±0.002 Hz, by direct observation, while making small adjustments to ω. Then we quasistatically changed ω to a desired ε, waited for at least a dozen phase slips (usually many more), and then acquired data using the camera and frame-grabber. After data acquisition at a particular ε, which might last several hours, we again determined $\omega_{ps}/2\pi$ by direct observation. For all experimental data reported below, we found $\omega_{ps}/2\pi$ before and after data acquisition to change by no more than 0.01 Hz and this translates to an uncertainty in ε of less than 1%.

III. FLOW REGIMES AT SMALL ε

Figure 2 is a schematic transition diagram for the different flow regimes observed for the hourglass geometry as the reduced Reynolds number ε is varied. The inner-hourglass base flow, like CCF is primarily azimuthal. However, the hourglass slightly modifies CCF by inducing a weak large-scale vortex pair, with each vortex filling half the system, and an inflow boundary at $z=0$. As the external driving is increased, two stationary *pairs* of Taylor vortices, reflection-symmetrically located about $z=0$, *gradually* appear. (Since it is equivalent to think of the pattern as consisting of a central vortex pair bounded by single vortices, we will sometimes refer to the central vortex pair.) Since there is no homogeneous section in the hourglass geometry, it is difficult to determine precisely the onset of TVF, which may well be an imperfect bifurcation given the presence of the large-scale vortices [19]. The Taylor vortices are only strongly present when a region of the hourglass approximately $2d_0$ wide is supercritical. The Taylor vortex pairs are axisymmetric, and thus the pattern which they form is quasi-one-dimensional. As the angular speed of the hourglass is increased, additional Taylor vortex pairs appear symmetrically about $z=0$, i.e., the supercritical region widens. The wavelength of vortex pairs decreases for pairs further from $z=0$, which is consistent with the decrease in gap size at greater $|z|$ in the hourglass geometry. The width of individual vortices alternates as the wavelength of pairs decreases, an effect observed by Ning, Ahlers, and Cannell in the ramped region of their sys-

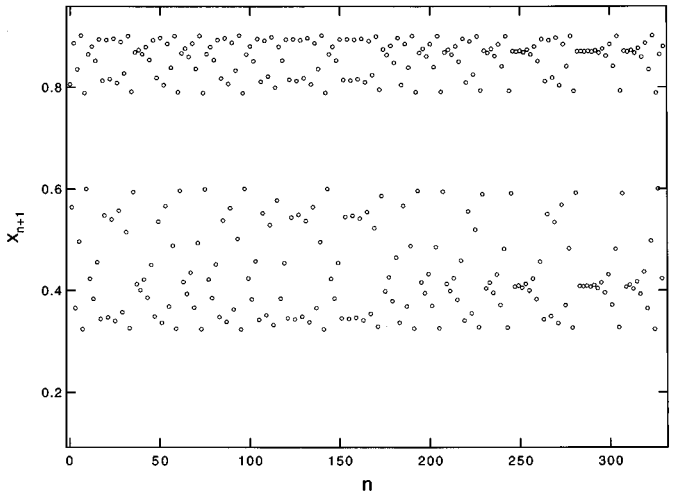

FIG. 6. x_{n+1} versus n with $\mu=3.6$, for the logistic-map $x_{n+1}=\mu x_n(x_n-1)$; $x_n \epsilon$ [0,1]. Note the similarity in the chevron patterns in this figure and in Fig. 5(d).

tem, which they attributed to large-scale flow caused by the ramp [14].

At a value of $\varepsilon=0$, for which the external driving is 10–15 % stronger than at the onset of TVF, there is a sharp transition to time-dependent periodic dynamics. This flow consists of diffusive axisymmetric drifting of vortices, during which the wavelength of vortex pairs expands. When the central vortex pair is stretched beyond the Eckhaus-stable limit, a phase slip is triggered that creates a new vortex pair, thereby restoring the pattern to Eckhaus stability. The entire process of diffusion and subsequent phase slip repeats itself periodically and involves the same Eckhaus-instability mechanism responsible for the period dynamics observed by Ning, Ahlers, and Cannell [14]. As ε increases in the periodic regime, the period decreases sharply. Figure 3(a) is a position-time diagram of the pattern just above the transition to periodic phase slips. The diagram is constructed, using 256 successive time frames set one second apart, of a column of pixels along the z direction, on which the intensity of light reflected off Kalliroscope flakes has been recorded. Only a portion of the system from $z=-4.0$ to 4.0, which includes the supercritical region, is shown, whereas the entire length of the system is from $z=-14.5$ to 14.5. The diagram shows that the time-dependent pattern breaks reflection symmetry, with the new vortex pair drifting to the right, and that the periodic phase slips occur each time at the same axial location near the midpoint of the system. To see this, note that the crests of the new vortex pair always emerge from the same respective locations. This pattern is similar to the model pattern of Riecke and Paap, in which periodic phase slips always occur less than one wavelength, and the same distance from, the symmetry center (for a given ε), but contrast with their results since the model's periodic dynamics are reflection-symmetric (phase slips alternate symmetrically about $z=0$) [16]. One possible explanation for broken symmetry in the physical system is the presence of finite ends which perturb the perfect symmetry of the model system. Figure 3(a) also shows that vortex pair creation occurs on a fast time scale compared to the time scale for vortex drifting and that the drift frequency of the new vortex pair is not constant, since its crests change direction.

At $\varepsilon=0.036$ there is a period-doubling transition to period-two dynamics in which the flow remains axisymmetric. An example of this pattern is shown in Fig. 3(b), which includes a wider region of the system than Fig. 3(a). The phase slips in the period-two regime alternate about $z=0$, with slightly different periods between right and left slips and broken reflection symmetry, as in the model of Riecke and Paap. Although the average time between phase slips in Fig. 3(b) is much smaller than in Fig. 3(a), there is no abrupt change in this time at the transition to period-two dynamics. The period has already decreased significantly between $\varepsilon=0$ and $\varepsilon=0.036$ and the average period continues to decrease slightly as ε is increased through the period-two regime. This suggests that the average drift frequency is both increasing as small ε increases and approaching a maximum, which is consistent with the periodic dynamics in the ramped system of Ning, Ahlers, and Cannell [14].

The next transition, at $\varepsilon=0.125$, is to a flow regime in which the quasi-one-dimensionality of the pattern is intermittently broken. The flow still includes diffusive axisymmetric drifting of vortices. However, rather than a rapid phase slip, the slow drifting triggers a process of vortex pair creation involving an excitation of spiral (i.e., nonaxisymmetric) vortices. Wimmer has observed spiral vortices in the flow between a rotating cone and cylinder, which is a similar geometry to the hourglass geometry [20]. The spiral excitations in our experiment are transient and their lifetimes irregular; sometimes an excitation dies out quickly and at other times it lasts on the same time scale as vortex drifting. Occasionally, there is an axisymmetric phase slip rather than a spiral excitation. After the spiral vortices die out, axisymmetric drifting begins anew, but the drifting time between excitations is also *aperiodic*. Thus, the dynamics of this regime are temporally chaotic, but intrinsically greater than one-dimensional. So they cannot be the chaotic dynamics predicted by the one-dimensional phase equation used in the model of Riecke and Paap. Instead, a spiral mode preempts the axisymmetric Eckhaus instability. The chaotic dynamics involving intermittent spiral excitations exist over a wide range of driving, until ε nears 0.50.

IV. PERIOD-DOUBLING CASCADE TO CHAOS

Chaotic dynamics can also be approached by decreasing ε from a regime of stationary Taylor vortices which exists above $\varepsilon=0.78$ (Fig. 2). At this higher ε, the Taylor vortices nearly fill the hourglass in the axial direction, but they are still bounded by subcritical regions. In the spatially ramped system used by Ning, Ahlers, and Cannell, there is also a restabilization of stationary Taylor vortices at higher ε: after the drift frequency of vortices between periodic phase slips reaches a maximum, it decreases to zero [14]. However, in their experiment the ramp fills with vortices and there is no longer any subcritical region, prior to restabilization. This suggests that a different mechanism is responsible for restabilization in our experiment than the one discussed by Paap and Riecke [9] to explain the data of Ning, Ahlers, and Cannell [21].

Below $\varepsilon=0.78$, the flow is time dependent. As can be seen in Fig. 2, there is a sequence of transitions from peri-

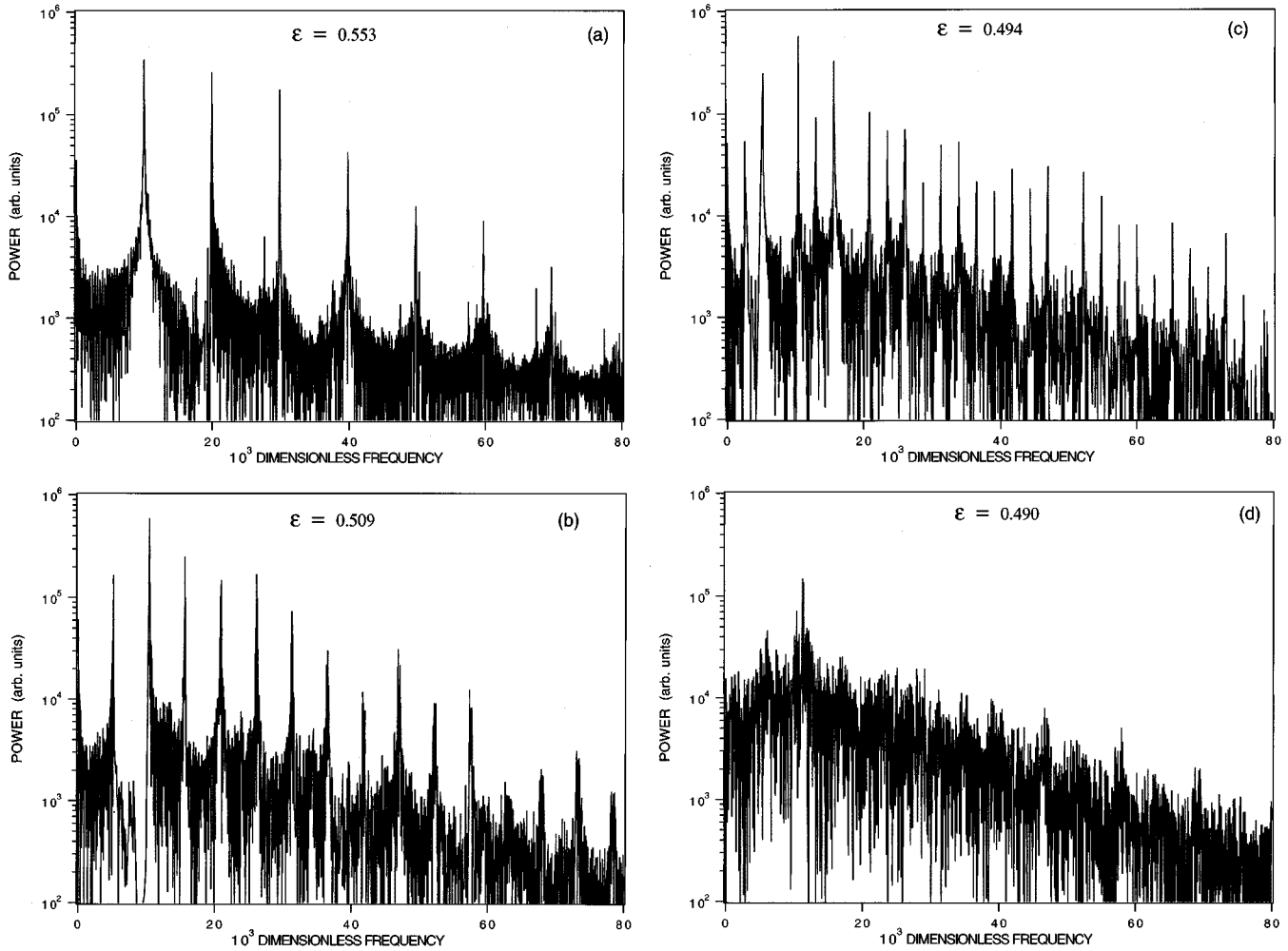

FIG. 7. Fast Fourier transforms from time series collected simultaneously with data for Fig. 5.

odic to period-two dynamics at $\varepsilon = 0.515$, to period-four dynamics at $\varepsilon = 0.499$, to chaotic phase slips at $\varepsilon = 0.493$. The flow in each of these regimes is axisymmetric and thus quasi-one-dimensional (with the exception of rare spiral excitations in the chaotic regime, to be discussed below). This sequence qualitatively agrees with the model results of Riecke and Paap, which show that a one-dimensional system with a reflection-symmetric ramp, which selects an Eckhaus-unstable state, can undergo a period-doubling cascade to spatiotemporal chaos. In this section, we present the details of our experimentally observed period-doubling cascade.

Our technique to determine when a phase slip occurred is to grab a column of pixel intensities every 0.2 s and then sum the pixel by pixel difference in intensity between columns separated by one second, so that we only save one number, representing the total difference, each fifth of a second. The reason for comparing time frames separated by one second is to allow enough time for a phase slip to occur between frames. Figure 4 is an example of this difference in intensity plotted against time. We identify when the phase slips occurred by the maximum of the peaks, which are typically four to five grabs wide and indicate a strong phase shift in the pattern. We repeatedly checked our method of determining phase slips by comparing to a time series of phase slips, recorded using direct observation, with typical agreement to 0.1 s for the time each slip occurred. Note that in Fig. 4 the period between phase slips alternates between two values, which is indicative of period-two dynamics. The periods are on the order of 20 s, i.e., 100 grabs, which was typical throughout our experiment.

In Fig. 5 we plot the dimensionless period T, representing the time between the nth$+1$ and nth phase slips versus n for periodic, period-two, period-four, and chaotic dynamics. T is scaled by $2\pi/\omega$, where ω is the angular speed of the hourglass at which the data was acquired. Periodic dynamics are evident in Fig. 5(a), in which data collected at $\varepsilon = 0.553$ show a mean period of 100.79 and a standard deviation of the mean $\sigma_m = 0.03$. In Fig. 5(b), with data taken at $\varepsilon = 0.509$, there is a period doubling in T, which alternates between two values. The filled circles represent even events with a mean of 89.25 and $\sigma_m = 0.04$ and the open circles represent odd events with a mean of 102.20 and $\sigma_m = 0.09$. Another doubling to period four is shown in Fig. 5(c), for which $\varepsilon = 0.494$ and each different symbol indicates T for every fourth event: open squares with mean 107.06 and $\sigma_m = 0.13$; filled squares with 100.51 and $\sigma_m = 0.13$; open circles with 88.38 and $\sigma_m = 0.05$; and filled circles with 87.87 and $\sigma_m = 0.06$. The plot shows a consistent sequence of four different periods. The split in the lesser two periods is

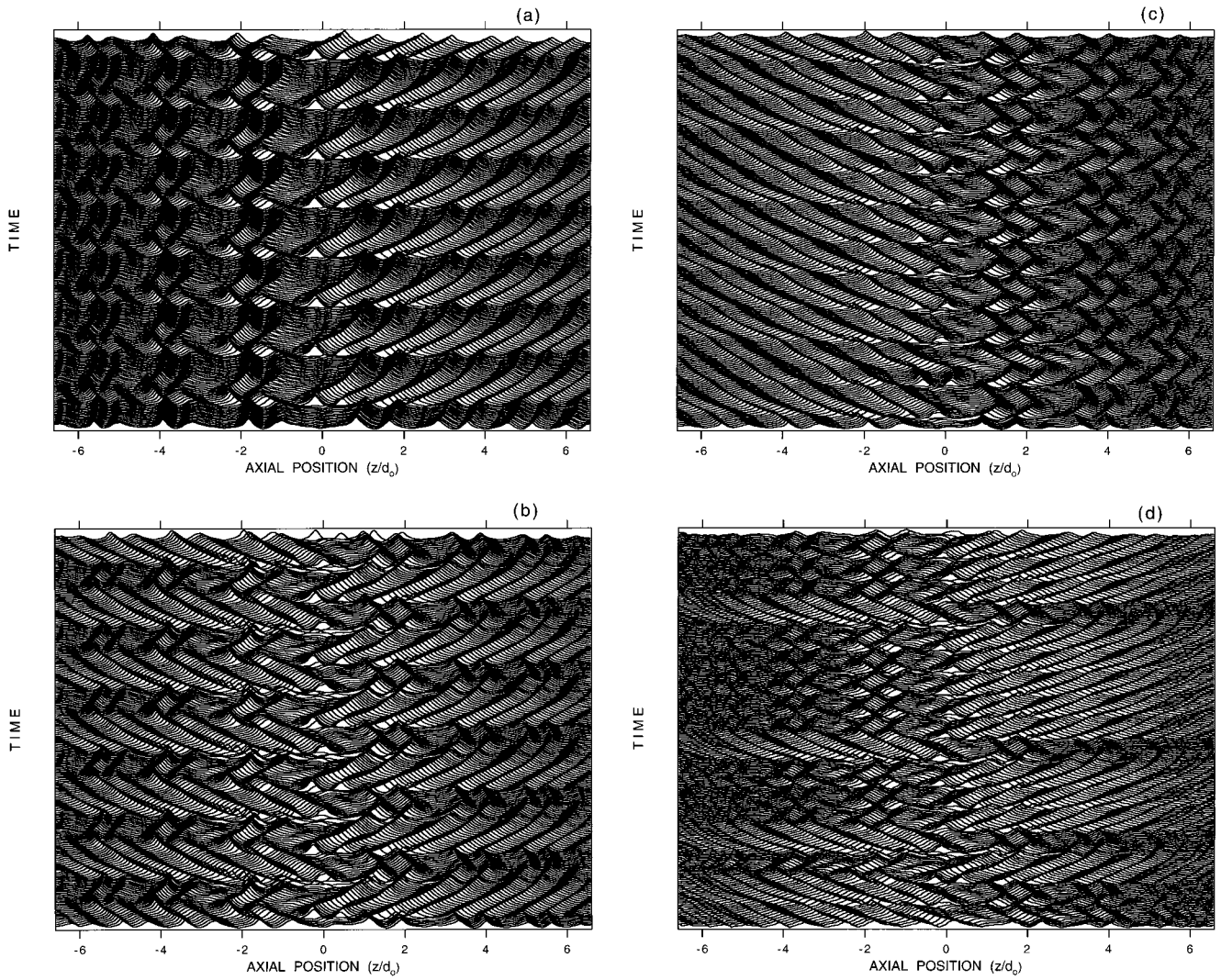

FIG. 8. Position-time diagrams, as in Fig. 3, for (a) periodic dynamics at $\varepsilon=0.708$, (b) period-two dynamics at $\varepsilon=0.508$, (c) period-four dynamics at $\varepsilon=0.495$, and (d) chaotic dynamics at $\varepsilon=0.491$.

small but discernible, with mean periods separated by a standard deviation ($\sigma=0.5$ for both lesser periods) and open circles almost always occurring with a slightly greater period than a neighboring, subsequent filled circle. Figure 5(d) with $\varepsilon=0.490$ shows temporally chaotic dynamics for which there is no periodicity and a large variation in T from less than 80 to almost 160. Remarkably, the noticeable v-shaped chevron pattern in Fig. 5(d), in which successive periods tend to get farther apart, is also found in the chaotic regime of the logistic map just after a period-doubling cascade. To illustrate this point, in Fig. 6 we plot x_{n+1} versus n for the logistic map in such a chaotic regime.

We also acquired time series of the intensity of light reflected off Kalliroscope flakes over a small area of pixels near $z=0$ at the same time data for determining T was acquired. In Fig. 7 we show the fast Fourier transforms of time series collected simultaneously with the data in Fig. 5. The time series consist of 8,192 points with an acquisition frequency of 1.36 Hz, for a total acquisition time of 1.67 h. The dimensionless frequency in the transforms is scaled by $\omega/2\pi$. Figure 7(a) shows periodic dynamics with a fundamental frequency of 9.94×10^{-3}, which corresponds to the period in Fig. 5(a). In Fig. 7(b) there is the appearance of a subharmonic, indicating a period doubling, with a frequency of 5.23×10^{-3}, which is the inverse of the sum of the periods in Fig. 5(b), as expected. Similarly, in Fig. 7(c) there is an additional subharmonic at 2.60×10^{-3}, which corresponds to the sum of the four periods in Fig. 5(c), giving further evidence of period-four dynamics. Figure 7(d) shows the noisy spectrum with no harmonics characteristic of chaotic-dynamics.

In Fig. 8 we show position-time diagrams of patterns in each of the four dynamic regimes, for a portion of the system from $z=-6.4$ to 6.4. The pattern for periodic dynamics in Fig. 8(a), at $\varepsilon=0.708$, is very similar to the pattern in Fig. 3(a) for periodic dynamics at small ε. Phase slips in the periodic regime always occur at the same location, with new vortex pairs always emerging from the central vortex pair, similar to the model results of Riecke and Paap. But the pattern is not reflection-symmetric, unlike the model pattern for periodic dynamics. The period-two pattern in Fig. 8(b) at $\varepsilon=0.508$, closely resembles the small ε period-two pattern

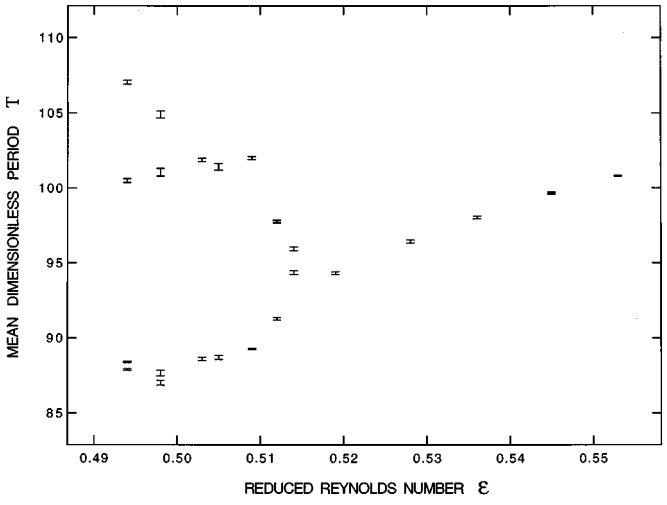

FIG. 9. Bifurcation diagram showing mean periods as a function of ε. Error bars indicate one standard deviation of the mean σ_m.

in Fig. 3(b), with broken reflection symmetry and alternating location and drifting direction for phase slips, as in the model. This supports one of the main conjectures of Riecke and Paap that a spatial ramp must induce an Eckhaus instability at multiple locations for period doublings, or chaos, to occur [15,16]. The period-four pattern shown for $\varepsilon = 0.495$ in Fig. 8(c) is quite intriguing in that phase slips no longer alternate in direction but, instead, newly created vortex pairs always drift to the left (which is opposite to the direction for periodic patterns). However, the location of the phase slips still alternates, as can easily be seen in Fig. 8(c). It is likely that there is a further small split in location for even and odd phase slips, respectively, indicative of period four, but these additional splittings cannot be resolved on the space and time scales of the diagram. The position-time diagram for $\varepsilon = 0.491$ in Fig. 8(d) shows spatially chaotic phase dynamics, since there is no periodicity in the location or direction of phase slips. However, the chaos is confined to the phase of the pattern and does not effect the underlying spatial organization of TVF. We even observed rare phase slips in the chaotic regime that emerge from a vortex pair neighboring the central vortex pair [this does not occur in Fig. 8(d)]. Apparently, the pattern has been Echkhaus destabilized over several wavelengths and there is a competition between phase slip processes that generates chaos, as in the model.

Figure 9 is a bifurcation diagram in which we plot mean T versus ε between 0.553 and 0.494 (this includes the periodic, period-two, and period-four, but not chaotic, regimes). The error bars indicate plus or minus one standard deviation of the mean. Mean periods were calculated for each different period at a particular ε. For example, we calculated four means, associated with the four periods in Fig. 5(c), at $\varepsilon = 0.494$. At each ε there were at least 75 phase slips recorded, and sometimes more than 300. The diagram shows two period-doubling bifurcations.

Figures 5 and 7–9 paint a picture of a period-doubling cascade to spatiotemporal chaotic phase dynamics. The periodic and period-doubled patterns are each quasi-one-dimensional, with axisymmetric vortex drifting and axisymmetric phase slips. In the chaotic regime, however, just beyond the transition from period-four phase slips, we observed occasional, brief spiral excitations temporally interspersed between axisymmetric phase slips. For example, seven of the 339 phase slips in Fig. 5(d) involved nonaxisymmetric excitations lasting about three seconds [22]. Since these departures from axisymmetry are rare and brief, it is plausible that this regime involves chaotic dynamics resulting from one-dimensional mechanisms and predicted by the phase equation used by Riecke and Paap. Indeed, this regime is qualitatively different from the chaotic dynamics in which spiral excitations are dominant and usually long-lived, which occurs at lower ε, although there is no sharp boundary between these two types of chaos. As indicated in Fig. 2, if ε is decreased below about 0.480, spiral excitations dominate. A spiral mode is competing with the Eckhaus instability and it appears that, at the transition to chaos dominated by axisymmetric phase slips (at $\varepsilon = 0.493$ just below the period-doubling cascade), the spiral mode is nearly equally unstable. It is the presence of an additional frequency associated with the spiral mode that possibly truncates the cascade at period four. There is theoretical evidence from Horner that a periodic perturbation eliminates the higher bifurcations of a period-doubling sequence in a one-dimensional map [23]. In the regime from $\varepsilon = 0.125$ to 0.480 dominated by intermittent spiral excitations, the spiral mode preempts the axisymmetric Eckhaus instability.

V. CONCLUSIONS

We have presented experimental evidence of a mechanism for the generation of chaos in a pattern-forming system. Our data demonstrate a sequence of period-doubling bifurcations leading to spatiotemporally chaotic phase dynamics in Taylor vortex flow with hourglass geometry, a subcritically ramped quasi-one-dimensional system, in qualitative agreement with the theoretical model of Riecke and Paap [15,16]. The hourglass geometry was chosen in order to fulfill the general conditions underlying the phase equation used in the model. The mechanism that generates chaotic phase dynamics is phase diffusion together with a ramp-induced Eckhaus instability, for which the pattern is destabilized over several wavelengths. The flow remains spatially organized even in the chaotic regime. Since phase diffusion and Eckhaus instability are features of many pattern-forming systems, it should be possible to observe chaotic phase dynamics in other systems (e.g., Rayleigh-Benard convection and viscous fingering) with appropriately chosen subcritical ramps. We also observed an intriguing chaotic regime, dominated by spiral excitations, in which axisymmetry is broken only intermittently.

ACKNOWLEDGMENTS

We wish to thank Professor Hermann Riecke and Professor Randall Tagg for useful discussions on this research. We also wish to thank Steve Attanasi for constructing the hourglass apparatus. This research was supported by Research Corporation and by the Murdock Charitable Trust.

[1] Y. Pomeau and P. Manneville, J. Phys. Lett. **40**, L609 (1979).
[2] M. Wu and C. D. Andereck, Phys. Rev. A, **43**, R2074 (1991).
[3] M. Wu and C. D. Andereck, in *Ordered and Turbulent Patterns in Taylor-Couette Flow*, edited by C. D. Andereck and F. Hayot (Plenum, New York, 1992).
[4] For a review of reduced nonlinear equations, see M. C. Cross and P. C. Hohenberg, Rev. Mod. Phys. **65**, 851 (1993).
[5] L. Kramer, E. Ben-Jacob, H. Brand, and M. C. Cross, Phys. Rev. Lett. **49**, 1891 (1982).
[6] D. S. Cannell, M. A. Dominguez-Lerma, and G. Ahlers, Phys. Rev. Lett. **50**, 1365 (1983).
[7] M. A. Dominguez-Lerma, D. S. Cannell, and G. Ahlers, Phys. Rev. A **34**, 4956 (1986).
[8] H. Riecke and H.-G. Paap, Phys. Rev. Lett. **59**, 2570 (1987).
[9] H.-G. Paap and H. Riecke, Phys. Fluids A **3**, 1519 (1991).
[10] For a review of bifurcations in Taylor-Couette flow, see R. C. DiPrima and H. L. Swinney, in *Hydrodynamic-Instabilities and Transitions to Turbulence*, edited by H. L. Swinney and J. P. Gollub (Springer, Berlin, 1981).
[11] For a review of pattern dynamics in Taylor-Couette flow, see R. Tagg, Nonlinear Sci. Today **4**, 1 (1994).
[12] W. Eckhaus, *Studies in Nonlinear Stability Theory* (Springer, New York, 1965).
[13] H. Riecke and H.-G. Paap, Phys. Rev. A **33**, 547 (1987).
[14] L. Ning, G. Ahlers, and D. S. Cannell, Phys. Rev. Lett. **64**, 1235 (1990).
[15] H. Riecke and H.-G. Paap, in *Ordered and Turbulent Patterns in Taylor-Couette Flow*, edited by C. D. Andereck and F. Hayot (Plenum, New York, 1992).
[16] H. Riecke and H.-G. Paap, Europhys. Lett. **14**, 433 (1991).
[17] I. Rehberg, E. Bodenschatz, B. Winkler, and F. H. Busse, Phys. Rev. Lett. **59**, 282 (1987).
[18] For a discussion on the properties of Kalliroscope, see P. Matisse and M. Gorman, Phys. Fluids **27**, 759 (1984).
[19] H. Riecke (private communication).
[20] M. Wimmer, Strömungsmech, Strömungsmasch. **44**, 59 (1992).
[21] Riecke and Paap argued that an entirely supercritical ramp provides a wider range of Eckhaus-stable states to accommodate the variation in wave number created by the ramp.
[22] The signature for spiral excitations in our plots of difference in intensity versus time is a broad jagged peak about three times wider than a smooth peak representing an axisymmetric phase slip.
[23] H. Horner, Phys. Rev. A **27**, 1270 (1983).